Desalination and Water Treatment
www.deswater.com
doi: 10.1080/19443994.2013.836991

52 (2014) 7766–7775
December

Taylor & Francis
Taylor & Francis Group

Removal of methylene blue from colored effluents by adsorption onto ZnAPSO-34 nanoporous material

B. Abbad[a,b,*], A. Lounis[b]

[a]*Water Treatment and Refrigeration by Renewable Energy, UDES, Solar Equipment Development Unit, Rte Nle N 11 Bou-Ismail 42415, Tipaza, Algeria*
Tel. +213 24410298; Fax: +213 24410484; email: babad80@yahoo.fr
[b]*USTHB, Science and Materials Engineering Laboratory, B.P. 32 El Alia, Algiers, Algeria*

Received 20 January 2013; Accepted 2 August 2013

ABSTRACT

The effects of equilibrium time, solution pH, and sorption temperature of cationic methylene blue (MB) adsorption on nanoporous metallosilicoaluminophosphate ZnAPSO-34 were studied using a batch equilibration method. UV–Vis spectroscopy was used to obtain the adsorption isotherms at 20°C. The optimum period for adsorption was 300 min. In fact, MB removal increased from 82 to 95% when we double the amount of adsorbent from 0.05 to 0.1 g l^{-1}. The equilibrium adsorption data were analyzed using Langmuir, Freundlich, and Temkin isotherm models. Langmuir isotherm was found to be the best-fitting model and the process followed pseudo-second-order kinetics. The results showed that ZnAPSO-34 could be employed as an alternative for the removal of dyes and colorants from aqueous solutions.

Keywords: Adsorption; Dye; Metallosilicoaluminophosphate; Methylene blue

1. Introduction

The growth of the world population in the last century, in addition to economic growth, the development of various industries and the use of fertilizers and pesticides in modern agriculture, has generated a significant quantity of hazardous waste, which is reflected in a considerable rise in both fresh water consumption and wastewater production. The effluents of wastewater in some industries such as dyestuff, textiles, leather, paper, and plastics contain various kinds of synthetic dyestuffs [1]. The textile industry, which is one of the largest water consumers in the world, produces wastewater comprising various recalcitrant agents such as dye, sizing agents, and dying aid. Removal of emerging contaminants of concern is now as ever important in the production of safe drinking water and the environmentally responsible release of wastewater. There are many conventional methods that can remove colored dyes from wastewater: chemical coagulation–flocculation, membrane technology, biological methods such as anaerobic/aerobic sequential processes, oxidative degradation by using chlorine or ozone, photo-degradation, and adsorption [2–6]. Hence, treatment of colored wastewater requires new adsorbents that are economical, easily available, and effective. There are several types of adsorbents being applied in industrial wastewater such as activated carbon, silica gel, and alumina [7–18]. Molecular sieves like aluminosilicate or aluminophosphate materials containing tiny pores of precise and uniform size, are used as adsorbents, catalyst carriers, desiccants, and so on [19–22].

*Corresponding author.

Zeolites, which are aluminosilicate members of the family of microporous solids known as "molecular sieves," have already found many applications because of its high cation-exchange capacity and surface area, etc. In recent years, synthetic and natural zeolites have become increasingly important due to the wide range of their chemical and physical properties and have been studied for the liquid adsorption of dissolved pollutants in water and/or wastewater. A lot of studies have focused on the adsorption of methylene blue a cationic dye by synthesized and natural zeolites [23–33]. The results showed that the adsorption kinetics and isotherms could be well described by the pseudo-second-order model and the two-parameter model (i.e. the Langmuir and Freundlich), respectively.

Among the AlPOs, the metalloaluminophosphates and metallosilicoaluminophosphates (MAPSOs) materials encompass the characteristics of both zeolites and aluminophosphates, which results in their unique catalytic, ion-exchange, and adsorbent properties [6,34–37].

To our knowledge, no previous reports have been made to investigate the adsorption performance of dyes on the synthetic MAPSOs.

For the purpose of serving it as an effective decolorizing adsorbent, ZnAPSO-34, a synthetic aluminophosphate material with the chabazite (CHA) structure[38], was prepared using hydrothermal synthesis in the present study and was also used as adsorbent for the adsorption of cationic dye in aqueous solution. The pore structure comprises eight member rings with 0.38 nm opening into large ellipsoidal cavities of 0.67–1.0 nm.

In this work, initial dye concentration, contact time, adsorbent dosage, pH, and kinetic studies were carried out to evaluate the adsorption capacity ZnAPSO-34 nanoporous material for the removal of MB from aqueous solutions.

2. Materials and methods

2.1. Preparation of zeotype for laboratory experiments

ZnAPSO-34 was synthesized by following previously reported procedure [39]. The typical synthesis gels with a molar composition of 0.8SiO2:0.8Al2O3: 1-P2O5:1TEAOH:0.4Zn:225H2O were prepared in 120-ml Teflon-lined autoclave. Isopropoxyde of alumina (Fluka) and ortho-phosphoric acid (Merck 85%) were used as aluminum and phosphorus sources, respectively; the divalent metal was introduced as acetate (zinc acetate, Fluka p.a.), other reactants were fumed silica (Aerosil 200, Serva), tetraethylammonium hydroxide (20% aqueous solution TEAOH, Fluka), and deionized water.

In order to obtain the final gel solution, isopropoxyde of alumina was slowly added to an aqueous solution containing ortho-phosphoric acid and the metal salt, while maintaining the mixture under magnetic stirring for 1 h. Then, the TEAOH solution is added, followed by the required amount of silica. The whole mixture is mixed by stirring for 2 h. The crystallization occurred under static conditions in an oven at 180–200 ℃ for 24 h. The autoclaves were cooled down to room temperature under running water, and the products were recovered by centrifugation, washed, and dried at 80 ℃ overnight.

The final product was a white powder. Finally, the product was calcined at 550 ℃ for 5 h at the rate of 1 ℃/min to remove the organic templates.

2.2. Preparation of basic dye solution

Methylene blue used was of analytical reagent grade and supplied by BIOCHEM Chemopharma (MW = 319.86 g, Absorption max (water):663–667 nm). Stock solutions of the test reagent were made by dissolving methylene blue, (3,9-bis dimethyl-aminophenazo thionium chloride), in distilled water. The structure of this dye is shown in Fig. 1.

All the other chemicals used were of analytical reagent grade and were purchased from Merck (Germany).

2.3. Batch sorption studies

2.3.1. Adsorption studies

The adsorption was performed by batch experiments. Kinetic experiments were carried out by stirring 250 ml of dye solution of known initial dye concentration with 0.05 g of ZnAPSO-34 at room temperature (20 ℃) at 400 rpm in different 500-ml PE flasks. At different time intervals, samples have been drawn out and then centrifuged at 3,500 rpm for 10 min. The concentration in the supernatant solution

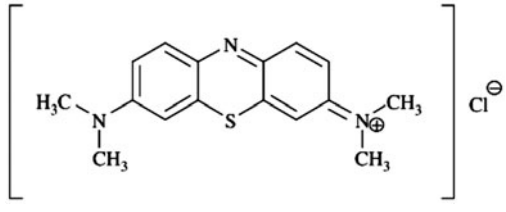

Fig. 1. Structure of methylene blue.

was analyzed using a UV spectrophotometer SHIMADZU 1800 by measuring absorbance at λ max = 664 nm and pH = 6. Adsorption isotherms were carried out by contacting 0.05 g of ZnAPSO-34 with 250 ml of methylene blue over the concentration ranging from 2 to 10 mg l^{-1}.

The effect of pH was observed by studying the adsorption of dye over a pH range of 2–10. The initial pH of the dye solution was adjusted by the addition of 0.1 N solution of hydrogen chloride (HCl) or sodium hydroxide (NaOH).

The amount of dye adsorbed per unit weight of adsorbent; q_t (mg g^{-1}) was calculated using the mass balance equation given by:

$$q_t = \frac{(C_0 - C_t)V}{m} \tag{1}$$

where C_0 (mg/l) is the initial dye concentration, C_t (mg/l) is the liquid-phase concentrations of dye at any time, V is the volume of the solution (l), and m is the mass of dry adsorbent used (g).

The dye removal percentage can be calculated as follows:

$$R(\%)_t = \frac{(C_0 - C_t)}{C_0} \times 100 \tag{2}$$

2.3.2. Error analysis

Due to the inherent bias resulting from the linearization of the isotherm and kinetic models, four different error functions of the nonlinear regression basin were employed as criteria for the quality of fitting [40].

2.3.2.1. The root mean square error. The root mean square error (RMSE) has been used by a number of researchers in the field to test the adequacy and accuracy of the model fit with the experimental data:

$$\mathrm{RMSE} = \sqrt{\frac{1}{n-2}\sum_{1}^{n}(q_i - q_{ie})^2} \tag{3}$$

where q_i is the experimental sorption capacity from the batch experiment i, $q_{ie,}$ is the sorption capacity estimated from the sorption model for corresponding q_i and n is the number of observations in the batch experiment.

2.3.2.2. The chi-squared test. The chi-squared test statistic is basically the sum of the squares of the differences between the experimental data and data obtained by calculating from models, with each squared difference divided by the corresponding data obtained by calculating from models. The chi-squared test has some similarity with the RMSE and is given as:

$$\chi^2 = \sum_{i=1}^{n}\frac{(q_i - q_{ie})^2}{q_{ie}} \tag{4}$$

2.3.2.3. The sum of the absolute errors. The sum of the absolute errors (SAEs) is given as:

$$\mathrm{SAE} = \sum_{i=1}^{n}\left|q_t - q_{ie}\right| \tag{5}$$

The isotherm parameters determined by this method provide a better fit as the magnitude of the errors increases, biasing the fit toward the high concentration data.

2.3.2.4. The average relative error. The average relative error (ARE) is defined as:

$$\mathrm{ARE} = \frac{100}{n}\sum_{i=1}^{n}\left|\frac{q_t - q_{ie}}{q_t}\right| \tag{6}$$

This error function attempts to minimize the fractional error distribution across the entire concentration range.

2.4. Characterization of the adsorbent

The as-synthesized product was characterized initially by X-ray powder diffraction using a diffractometer (Miniflex2, RIGAKU) equipped with a linear position sensitive detector (CuKa1 radiation, $k = 1.5406$ Å). The morphology and average size of the crystals were determined by scanning electron microscopy (SEM) using a HITACHI S4800 microscope.

Elemental composition of the products (Al, P, Si, and Zn) was determined by using JEOL 5800 SEM with energy dispersive X-ray analyzer attachment (EDX).

3. Results and discussion

3.1. Characterization of the adsorbent

The crystallinity of the sample and the phase identification were evaluated from XRD patterns (Fig. 2). Examination of the powder data of the sample revealed that only one phase was identified, which corresponds to CHA structure [41].

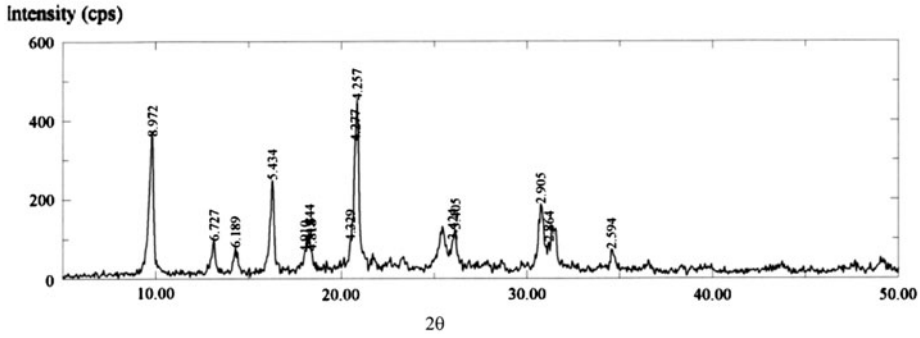

Fig. 2. X-ray powder diffraction of as calcined sample at 500°C.

We have examined the sample by SEM, looking for the morphology of the crystals. SEM images of the calcined samples are provided in Fig. 3. The sample prepared shows the typical CHA morphology: Cubic crystals are well developed in the size range of 3–10 μm.

The EDX analysis (Fig. 4) identified the characteristic peaks of all the elements present in the respective compositions (see Table 1).

3.2. Effect of various parameters on the MB adsorption

3.2.1. Effect of contact time and initial dye concentration

Equilibration time is an important parameter for economical wastewater treatment. The effects of contact time and initial dye concentration on removal are shown in Fig. 5. The results showed that kinetics of adsorption of MB consisted of two phases: an initial rapid phase where adsorption was fast and contributed significant to equilibrium uptake and a slower second phase whose contribution to the total MB adsorption was relatively small. The first phase was the instantaneous adsorption stage or external surface

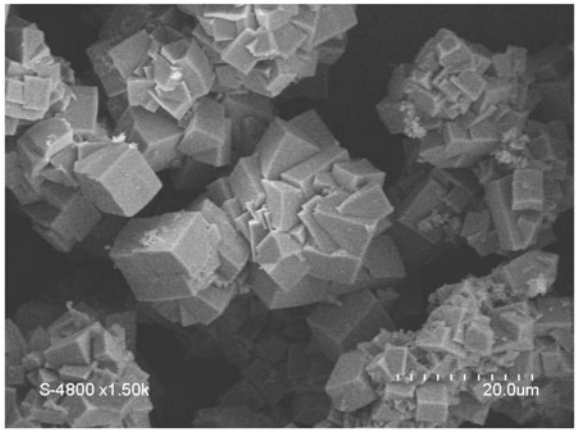

Fig. 3. SEM image of characteristic ZnAPO-34 crystals.

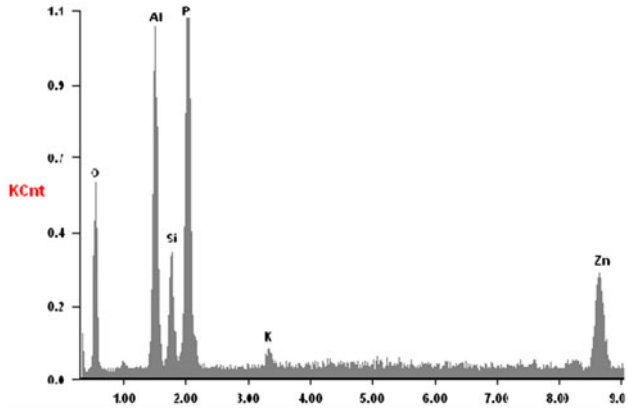

Fig. 4. EDX results in the analysis of ZnAPSO-34.

Table 1
Elemental composition (Wt %) of ZnAPSO-34

Element	O K	Al K	Si K	P K	K K	Zn K
Wt%	17.87	16.60	06.68	21.50	0.091	21.19

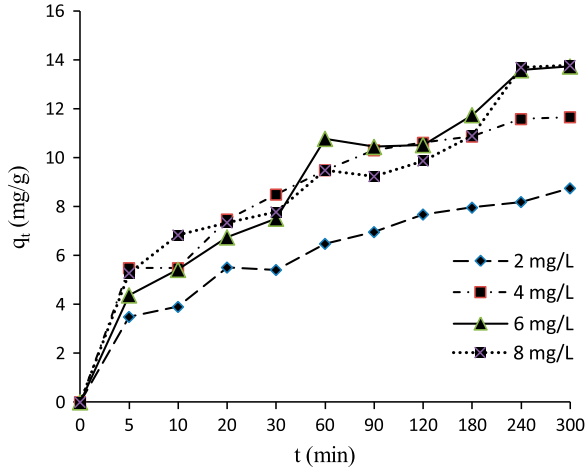

Fig. 5. Effect of initial dye concentration and contact time on the adsorption of methylene blue onto ZnAPSO-34.

adsorption. The second phase was the gradual adsorption stage, and finally, the MB uptake reached equilibrium. Equilibrium adsorption was established within 300 min for all concentrations.

These results show that the contact time required for maximum uptake of the dye by ZnAPSO-34 was strongly dependent on initial methylene blue concentration. The results also show that the amount of methylene blue adsorbed increased with an increase in initial dye concentration.

3.2.2. Effect of adsorbent dose

The effects of adsorbent dosage on MB removal are presented in Fig. 6. Removal efficiency increased from 85 to 94% with an increase in the dosage from 0.05 to 0.1 g l^{-1} and then remained almost constant. This was caused by the fact that, with increasing adsorbent dosage, more adsorption sites are available. However, increasing the sites had little effect on removal efficiency at high adsorbent dosage because of the establishment of equilibrium at an extremely low adsorbate concentration in the solution before reaching saturation. It can also be seen from Fig. 6 that the MB removal efficiency changed slightly from 85 to 97% with an increase in adsorbent dosage from 0.1 to 0.25 g l^{-1}. This result is mainly because the adsorption sites were more or less saturated by MB at low adsorbent doses (<0.1 g l^{-1}), but unsaturated at high doses (>0.25 g l^{-1}). The adsorbent dosage was fixed at 0.05 g l^{-1} for the remaining experiments.

3.2.3. Effect of pH

The pH is one of the most important factors controlling the adsorption of dye on to adsorbent. Change

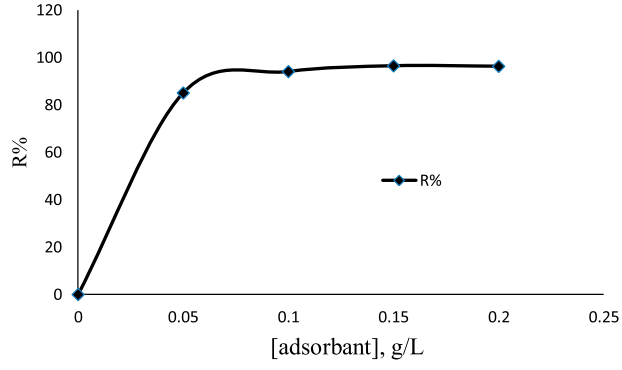

Fig. 6. Effect of adsorbent dosage on the adsorption of methylene blue onto ZnAPSO-34 (dye concentration: 2 mg l^{-1} temperature: 293 K; contact time: 300 min) pH: 6.

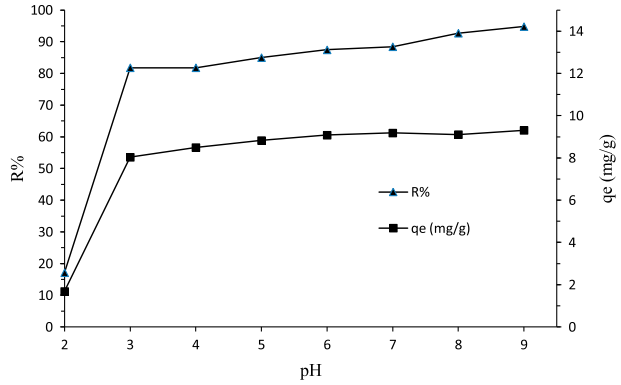

Fig. 7. Effect of pH on the adsorption of MB on ZnAPSO-34 (Initial dye concentration: 2 mg/L).

of the pH affects the adsorptive process through dissociation of functional groups on the adsorbent surface active sites. The pH of dye solution may also change the molecular structure of dye, and therefore, the removal of ionic dye can be influenced greatly.

The effect of pH on the adsorption of methylene blue by ZnAPSO-34 is shown in Fig. 7.

The dye uptake was found to increase with increasing pH, and it increased from 1.68 to 9.31 mg/g for an increase in pH from 2 to 9. The methylene blue adsorption by ZnAPSO-34 was significantly affected over the pH range of 2–4. At higher pH values (5–9), the adsorbed amount of MB almost kept constant. This can be explained by considering the electrostatic attraction that exists between the negatively charged surface of the adsorbent and MB, a cationic dye. The surface of ZnAPSO-34 may contain a large number of active sites, and the solute (dye ions) uptake can be related to the active sites and also to the chemistry of the solute in the solution. The results may be attributed to the following factors. At lower pH values, hydrogen ion competes with MB cation, and most of the carboxyl of adsorbent exists in the form of –COOH, which reduce the adsorbed amounts for MB. At higher pH values, more hydroxyls and $–COO^-$ occur, which may enhance electrostatic attraction and the adsorption capacity of adsorbent for MB. Similar phenomena were reported by many researchers [24,42,43].

3.2.4. Adsorption kinetics

It is important to be able to predict the rate at which contamination is removed from aqueous solutions in order to design an adsorption treatment plant. In order to investigate the adsorption processes MB dyes on ZnAPSO-34, two kinetic models were

Table 2
Kinetic parameters for the adsorption of MB on ZnAPSO-34

Models	Parameters	$[BM]_{initial} = 2\,mg/l$	$[BM]_{initial} = 4\,mg/l$	$[BM]_{initial} = 6\,mg/l$	$[BM]_{initial} = 8\,mg/l$
Pseudo-second order	R^2	0.995	0.997	0.981	0.999
	$k_2(g\,mg^{-1}\,min^{-1})$	5.97×10^{-3}	5.88×10^{-3}	4.18×10^{-3}	5.06×10^{-3}
	$q_e$cal $(mg\,g^{-1})$	8.775	11.728	13.101	14.238
	q_e exp$(mg\,g^{-1})$	8.75	11.66	13.73	13.78
	χ^2	0.023	0.053		0.203
	RMSE	0.197	0.400		0.876
Pseudo-first order	R^2	0.980	0.976	0.960	0.972
	$k_1(g\,mg^{-1}\,min^{-1})$	0.028	0.039	0.054	0.066
	q_e cal $(mg\,g^{-1})$	8.75	11.66	13.73	13.78
	χ^2	7.438	6.356	5.782	8.505
	RMSE	1.089	1.326	2.618	3.131

used: Lagergren first-order model [44] and Ho' pseudo-second-order model [45]. These models are most commonly used to describe the sorption of dyes as well as other pollutants (heavy metals) on solid sorbents. Parameters of the kinetic models were estimated from the experimental data with the aid of the nonlinear curve-fitting procedure.

The following expressions were used to describe two models, respectively:

$$\ln(q_e - q_t) = \ln q_e - k_1 t \tag{7}$$

$$\frac{t}{q_t} = \frac{1}{k_2 q_e^2} + \frac{t}{q_e} \tag{8}$$

where q_t and q_e are the amount of MB adsorbed on the adsorbents $(mg\,g^{-1})$ at time t and at equilibrium, respectively, k_1 (min^{-1}) and k_2 $(g\,mg^{-1}\,min^{-1})$ are the rate constants of first order and second order, respectively.

All the parameters of kinetics models are listed in Table 2. As can be seen in Table 2, the correlation coefficient, R^2 of pseudo-second-order kinetic model was greater than 0.99 for both MB solutions. Therefore, the calculated q_e values agreed with the experimental q_e values, implying that the adsorption kinetic of MB is well described by pseudo-second-order model.

From Table 2, it can be seen that the pseudo-second-order kinetic rate constants decreased with the increasing of initial MB concentrations. This is due to the competition for the adsorbent active sites are increased at higher concentration, and consequently, the adsorption rate will become slower.

Intraparticle diffusion model is an empirical functional relationship, assuming that the adsorption capacity varies almost proportionally with $t_{0.5}$ [41]:

$$q_t = k_{dif} t^{0.5} + C \tag{9}$$

where k_{dif} was the intraparticle diffusion rate constant $(mol\,s^{-1/2}\,g^{-1})$, and C was the intercept of the plot of q_t vs. $\sqrt{t}$.

The adsorbate transport from the solution to the surface of the adsorbent occurs in several steps. This phenomenon may be controlled by one or more steps such as film or external diffusion, pore diffusion, surface diffusion and adsorption on the pore surface, or a combination of more than one step through the adsorption process. It can be seen from Fig. 8 that the sorption process tended to follow two distinct phases.

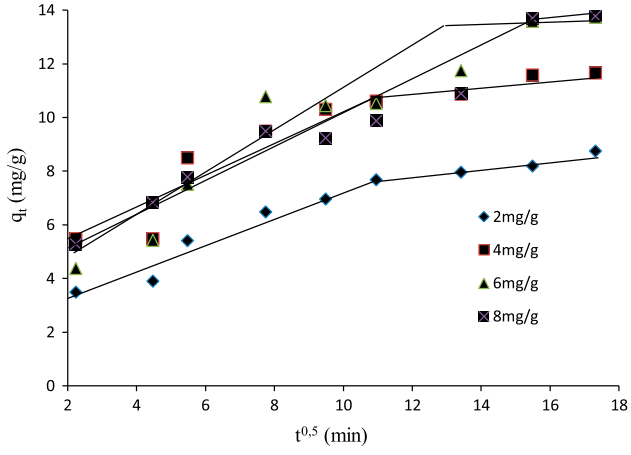

Fig. 8. Intraparticle diffusion model for the adsorption of MB onto ZnAPSO-34 at different initial concentrations.

The diffusion rate constant for the second step was much smaller than that of the first step. The first sharper step was the external surface adsorption (migration of dye from bulk of the solution to the surface of the adsorbent), and the second step was the gradual adsorption.

In addition, the pore size could also play a role in adsorption [29]. During adsorption process, MB can be adsorbed on the surface of aluminophosphate or move through the pores of the aluminophosphate mass. Diffusion was faster through the pores and was retarded when MB molecules moved through the smaller diameter channels. MB is an organic compound having a larger molecular size ($17.0 \times 7.6 \times 3.25$ Å), thus making it difficult to diffuse into pores of the aluminophosphate (ZnAPSO-34).

3.2.5. Adsorption isotherms

Adsorption isotherms are critical in optimizing the use of adsorbents and describe how adsorbate interacts with adsorbent. The analysis of the isotherm data with either theoretical or empirical equations is important to develop an equation which accurately represents the results and which could be used for design [42–44]. Several isotherms equations are available. Three of them have been selected in this study: Langmuir, Temkin, and Freundlich isotherms.

3.2.5.1. Langmuir isotherm. The Langmuir adsorption isotherm has been successfully applied to many pollutants adsorption processes and has been the most widely used sorption isotherm for the sorption of a solute from a liquid solution [42]. The saturated monolayer isotherm can be represented as

$$q_e = \frac{q_m K_L C_e}{1 + K_L C_e} \tag{10}$$

The above equation can be rearranged to the common linear form:

$$\frac{1}{q_e} = \frac{1}{K_L q_m} \times \frac{1}{C_e} + \frac{1}{q_m} \tag{11}$$

where C_e is the equilibrium concentration ($mg\,l^{-1}$); q_e is the amount of MB adsorbed per unit mass of zeolite ($mg\,g^{-1}$); q_m is q_e for a complete monolayer ($mg\,g^{-1}$), a constant related to sorption capacity; and K_L is a constant related to the affinity of the binding sites and energy of adsorption ($l\,mg^{-1}$).

3.2.5.2. Temkin isotherm. The derivation of the Temkin isotherm assumes that the fall in the heat of adsorption is linear rather than logarithmic, as implied in the Freundlich equation. The Temkin isotherm [43]:

$$q_e = A + B \ln C_e \tag{12}$$

where A and B are isotherm constants.

3.2.5.3. Freundlich isotherm. Freundlich isotherm is an empirical equation describing adsorption onto a heterogeneous surface. The Freundlich isotherm is commonly presented as [44]:

$$q_e = K_F C_e^{1/n} \tag{13}$$

where K_F and n are the Freundlich constants related

Table 3
Isotherm parameters for the adsorption of methylene blue on ZnAPSO-34

Models Parameters	Langmuir	Temkin	Freundlich
χ^2	0.1749	6.978	0.0457
R^2	0.997	0.960	0.975
q_{max} ($mg\,g^{-1}$)	14,492	–	–
b ($l\,mg^{-1}$)	4.059	1.867	–
R_L	0.046		
K_f ($mg^{1-1/n}\,g^{-1}\,l^{1/n}$)	–	–	10.804
$1/n$	–	–	0.168
K_T ($l\,mg^{-1}$)	–	6.646×10^{-4}	–
SAE	2.1558	21.827	1.2108
ARE	0.8481	5.0877	0.3693
RMSE	0.9307	7.808	0.5538

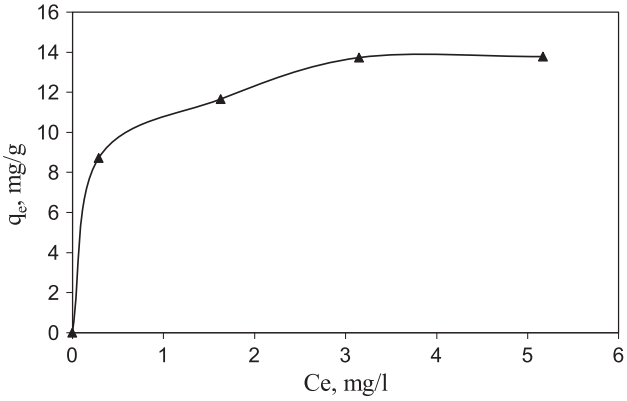

Fig. 9. Equilibrium isotherm of methylene blue onto ZnAPSO-34.

Table 4
Comparison of the adsorption capacities of various adsorbents for methylene blue dye

Dye	Adsorbent	q_{max} (mg g^{-1})	References
Fly ash-derived zeolites	Methylene blue	12.64	[48]
Clinoptilolite	Methylene blue	19.9	[49]
ZSM-5 zeolite	Methylene blue	6.41	22
ZnAPSO-34	Methylene blue	14.49	This work
Wheat shells	Methylene blue	16.56–21.50	51
Activated carbon	Methylene blue	435	52

to the adsorption capacity and adsorption intensity of the sorbent respectively. Eq. (12) can be linearized by taking logarithms:

$$\ln q_e = \ln K_F + \frac{1}{n} \ln C_e \quad (14)$$

From Table 3, it can be observed that the calculated isotherm parameters and their corresponding RMSE, ARE, SAE, and χ^2 values vary for the three linearized types of isotherms. It can be seen that the Freundlich model yields a better fit than the Langmuir and Temkin model, as reflected by a RMSE and χ^2 values. Freundlich isotherm showed better fit followed by Langmuir isotherms.

Correlation coefficient (R^2) shows that the Langmuir model is better than the Freundlich model in simulation of the adsorption isotherm. The agreement of the Langmuir model with the experimental results suggests that a monolayer coverage of MB on the outer surface of the adsorbent.

The essential feature of the Langmuir isotherm can be expressed by means of "R_L", a dimensionless constant referred to as separation factor or equilibrium parameter. R_L is calculated using the following equation [12,45]:

$$R_L = \frac{1}{1 + K_L C_0} \quad (15)$$

where C_0 is the highest initial dye concentration (mg L^{-1}). The value of R_L calculated as above equation is incorporated in Table 3. The value of R_L indicated the type of isotherm to be irreversible ($R_L = 0$), favorable ($0 < R_L < 1$), linear ($R_L = 1$), or unfavorable ($R_L > 1$). Further, the R_L value for MB onto ZnAPSO-34 at 20 °C is 0.046, and therefore, its adsorption is favorable.

The adsorption isotherm of methylene blue onto ZnAPSO-34 is presented in Fig. 9. The isotherm shows the "L" type-2 shape according to the classification of Giles [46], which indicate the great affinity of the MB toward the solid adsorbent. Furthermore, the shape of this isotherm is consistent with type I isotherm characterizes microporous adsorbents in the case of a gas-phase process as reported by Brunauer, Deming, Deming, and Teller [47], suggesting that the adsorption occurs on specific sites forming a monolayer. Type I isotherm correspond to nonporous or microporous solids with corresponding pore of diameters lower than 20 Å.

The L or Langmuir shape of the isotherms also means that there is no strong competition between the solvent and the adsorbate to occupy the adsorbent sites.

Table 4 compares the adsorption capacity ZnAPSO-34 with other adsorbents reported before [22,48–51]. As seen activated carbon generally has a high adsorption capacity for MB. ZnAPSO-34 shows a higher adsorption capacity than natural and synthesis zeolites and comparable capacity to wheat shells fly ash-derived zeolites.

4. Conclusion

This study indicated that ZnAPSO-34 has the potential to act as adsorbents for the removal of MB cationic dye from aqueous solutions. The analysis by SEM and EDX showed that the adsorbent material has a microporous structure, and it consists mainly of Al, P, Si, and Zn. The equilibrium adsorption isotherms have been validated in detail by Langmuir and Freundlich and Temkin models. The conditioning time of 3 h was found to be sufficient for reaching equilibrium. The rate of adsorption was found to conform to pseudo-second-order kinetics with a good correlation. Equilibrium data fitted very well in the Langmuir isotherm equation, confirming the monolayer adsorption capacity of methylene blue onto ZnAPSO-34 with a monolayer adsorption capacity of 14.49 mg/g. The dimensionless separation factor (R_L) showed that ZnAPSO-34 can be used for removal of methylene blue from aqueous solutions.

References

[1] E. Forgacs, T. Cserhati, G. Oros, Removal of synthetic dyes from wastewaters: A review, Environ. Int. 30 (2004) 953–971.

[2] G. Crini, Non-conventional low-cost adsorbents for dye removal: A review, Bioresour. Technol. 97 (2006) 1061–1085.

[3] T. Robinson, G. McMullan, R. Marchant, P. Nigam, Remediation of dyes in textile effluent: A critical review on current treatment technologies with a proposed alternative, Bioresour. Technol. 77 (2001) 247–255.

[4] M. Rafatullah, O. Sulaiman, R. Hashim, A. Ahmad, Adsorption of methylene blue on low-cost adsorbents: A review, J. Hazard. Mater. 177 (2010) 70–80.

[5] Y.S. Al-Degs, M.I. El-Barghouthi, A.A. Issa, M.A. Khraisheh, G.M. Walker, Sorption of Zn(II), Pb(II), and Co(II) using natural sorbents: Equilibrium and kinetic studies, Water res. 40 (2006) 2645–2658.

[6] N.N. Tusar, V. Kaucic, Nanoporous materials: From catalysis and hydrogen storage to wastewater treatment, Acta Chim. Slov. 53 (2006) 117–135.

[7] Ö. Yavuz, A.H. Aydin, Removal of direct dyes from aqueous solution using various adsorbents, Pol. J. Environ. Stud. 15(1) (2006) 155–161.

[8] S. Wang, H. Li, Dye adsorption on unburned carbon: Kinetics and equilibrium, J. Hazard. Mater. B126 (2005) 71–77.

[9] J.S. Piccin, C.S. Gomes, L.A. Feris, M. Gutterres, Kinetics and isotherms of leather dye adsorption by tannery solid waste, Chem. Eng. J. 183 (2012) 30–38.

[10] A. Gil, F.C.C. Assis, S. Albeniz, S.A. Korili, Removal of dyes from wastewaters by adsorption on pillared clays, Chem. Eng. J. 168 (2011) 1032–1040.

[11] N. Ouazene, A. Lounis, Adsorption characteristics of CI Basic Blue 3 from aqueous solution onto Aleppo pine-tree sawdust, Color. Technol. 128 (2011) 21–27. doi: 10.1111/j.1478-4408.2011.00327.x.

[12] M-C. Shih, Kinetics of the batch adsorption of methylene blue from aqueous solutions onto rice husk: Effect of acid-modified process and dye concentration, Desalin. Water Treat. 37 (2012) 200–214. doi: 10/5004/dwt.2012.1133.

[13] M. Belhachemi, F. Addoun, Adsorption of congo red onto activated carbons having different surface properties: Studies of kinetics and adsorption equilibrium, Desalin. Water Treat. 37 (2012) 122–129. doi: 10/5004/dwt.2012.2608.

[14] R. Hoppe, Gi. Schulz-Ekloff, D. Wohrle, E.S. Shpiro, O.P. Tkachenko, X.p.s. investigation of methylene blue incorporated into faujasites and AIPO family molecular sieves, Zeolites 13 (1993) 222–228.

[15] C. Hua, R. Zhang, L. Li, X. Zheng, Adsorption of phenol from aqueous solutions using activated carbon prepared from crofton weed, Desalin. Water Treat. 37 (2012) 230–237.

[16] M. Dogan, Y. Ozdemir, M. Alkan, Adsorption kinetics and mechanism of cationic methyl violet and methylene blue dyes onto sepiolite, Dyes Pigm. 75 (2007) 701–713.

[17] N. Barka, S. Qourzal, A. Assabbanei, A. Nounah, Y. Ait-Ichou, Adsorption of disperse blue SBL dye by synthesized poorly crystalline hydroxyapatite, J. Environ. Sci. 20 (2008) 1268–1272.

[18] S. Wang, H. Li, L. Xu, Application of zeolite MCM-22 for basic dye removal from wastewater, J. Colloid Interface Sci. 295 (2006) 71–78.

[19] A. Nicolas, S. Devautour-Vinot, G. Maurin, J.C. Giuntini, F. Henn, Cation dynamics upon adsorption of methanol in Na – Y faujasite type zeolites: A dielectric relaxation spectroscopy investigation, J. Phys. Chem. C 111 (2007) 4722–4726.

[20] M.A.S.D. Barros, A.S. Zola, P.A. Arroyo, E.F. Sousa-Aguiar, C.R.G. Tavares, Binary ion exchange of metal ions in y and x zeolites, Braz. J. Chem. Eng. 20(4) (2003) 413–421.

[21] S.B. Wang, Z.H. Zhu, Characterisation and environmental application of an Australian natural zeolite for basic dye removal from aqueous solution, J. Hazard. Mater. 136 (2006) 946–952.

[22] X. Jin, M-Q. Jiang, X-Q. Shan, Zh-G. Pei, Z. Chen, Adsorption of methylene blue and orange II onto unmodified and surfactant-modified zeolite, J. Colloid Interface Sci. 328 (2008) 243–247.

[23] F. Ferrero, Adsorption of methylene blue on magnesium silicate: Kinetics, equilibria and comparison with other adsorbents, J. Environ. Sci. 22(3) (2010) 467–473.

[24] R. Han, J. Zhang, P. Han, Y. Wang, Z. Zhao, M. Tang, Study of equilibrium, kinetic and thermodynamic parameters about methylene blue adsorption onto natural zeolite, Chem. Eng. J. 145 (2009) 496–504.

[25] C. Wang, J. Li, L. Wang, X. Sun, J. Huang, Adsorption of dye from wastewater by zeolites synthesized from fly ash: Kinetic and equilibrium studies, Chin. J. Chem. Eng. 17(3) (2009) 513–521.

[26] W.T. Tsai, K.J. Hsien, H.C. Hsu, Adsorption of organic compounds from aqueous solution onto the synthesized zeolite, J. Hazard. Mater. 166 (2009) 635–641.

[27] Sh. Sohrabnezhad, A. Pourahmad, Comparison absorption of new methylene blue dye in zeolite and nanocrystal zeolite, Desalination 256 (2010) 84–89.

[28] M. Akgül, A. Karabakan, Promoted dye adsorption performance over desilicated natural zeolite, Microporous Mesoporous Mater. 145 (2011) 157–164.

[29] T.S. Jamil, H.H. Abdel Ghafar, H.S. Ibrahim, I.H. Abd El-Maksoud, Removal of methylene blue by two zeolites prepared from naturally occurring Egyptian kaolin as cost effective technique, Solid State Sci. 13 (2011) 1844–1851.

[30] D.A. Fungaro, M. Bruno, L.C. Grosche, Adsorption and kinetic studies of methylene blue on zeolite synthesized from fly ash, Desalin. Water Treat. 2 (2009) 231–239.

[31] X. Qi, J. Li, T. Ji, Y. Wang, L. Feng, Y. Zhu, X. Fan, C. Zhang, Catalytic benzene hydroxylation over copper-substituted aluminophosphate molecular sieves (CuAPO-11), Microporous Mesoporous Mater. 122 (2009) 36–41.

[32] Z. Lounis, A. Riahi, F. Djafri, J. Muzart, Chromium-exchanged zeolite (Cr E-ZSM-5) as catalyst for alcohol oxidation and benzylic oxidation with t-BuOOH, Appl. Catal., A 309 (2006) 270–272.

[33] Ch. Baerlocher, L.B. McCusker, D.H. Olson, Atlas of Zeolite Framework Types, 6th revised ed., Elsevier, Amsterdam, 2007.

[34] G. McKay, M.J. Bino, A.R. Altamemi, The adsorption of various pollutants from aqueous solutions on to activated carbon, Water res. 19(4) (1985) 491–495.

[35] S. Kundu, A.K. Gupt, Arsenic adsorption onto iron oxide-coated cement (IOCC): Regression analysis of equilibrium data with several isotherm models and their optimization, Chem. Eng. J. 122 (2006) 93–106.

[36] R. Han, Y. Wang, W. Zou, Y. Wang, J. Shi, Comparison of linear and nonlinear analysis in estimating the Thomas model parameters for methylene blue adsorption onto natural zeolite in fixed-bed column, J. Hazard. Mater. 145 (2007) 331–335.

[37] M.M.J. Treacy, J.B. Higgins, Collection of Simulated XRD Powder Patterns for Zeolites, 4th revised ed., Elsevier, Amsterdam, 2001.

[38] L. Wang, J. Zhang, A. Wang, Removal of methylene blue from aqueous solution using chitosan-g-poly(acrylic acid)/montmorillonite superadsorbent nanocomposite, Colloids Surf., A 322 (2008) 47–53.

[39] S. Lagergren, Zur theorie der sogenannten adsorption gelosterstoffe [About the theory of so-called adsorption of soluble substances], Kungliga Svenska Vetenskapsakademiens. Handlingar 24(4) (1898) 1–39.

[40] Y.S. Ho, G. Mckay, A comparison of chemisorption kinetic models applied to pollutant removal on various sorbents, Inst. Chem. Eng Trans. IChemE, Part B 76 (1998) 332–340.

[41] W.J. Weber, J.C. Morris, Kinetics of adsorption on carbon from solution, J. Sanit. Eng. Div. ASCE 89 (1963) 31–59.

[42] I. Langmuir, The constitution and fundamental properties of solids and liquids, J. Am. Chem. Soc. 40 (1918) 1361–1403.
[43] M.J. Temkin, V. Pyzhev, Recent modifications to Langmuir isotherms, Acta Phys. chim. 12 (1940) 217–222.
[44] H.M.F. Freundlich, Over the adsorption in solution, J. Phys. Chem. 57 (1906) 385–470.
[45] K.G. Bhattacharyya, A. Sharma, Kinetics and thermodynamics of methylene blue adsorption on Neem (*Azadirachta indica*) leaf powder, Dyes Pigm. 65 (2005) 51–59.
[46] H. Giles, D. Smith, A. Huitson, A general treatment and classification of the solute adsorption isotherm. I. Theoretical, J. Colloid Interface Sci. 47 (1974) 755–765.
[47] S. Brunauer, L.S. Deming, W.E. Deming, E.J. Teller, On a theory of the van der Waals adsorption of gases, Am. Chem. Soc. 62 (1940) 1723–1732.
[48] S. Wang, Y. Boyjoo, A. Choueib, A comparative study of dye removal using fly ash treated by different methods, Chemosphere 60(10) (2005) 1401–1407.
[49] S. Wang, Y. Peng, Natural zeolites as effective adsorbents in water and wastewater treatment, Chem. Eng. J. 156 (2010) 11–24.
[50] Y. Bulut, H. Aydın, A kinetics and thermodynamics study of methylene blue adsorption on wheat shells, Desalination 194 (2006) 259–267.
[51] N. Kannan, M.M. Sundaram, Kinetics and mechanism of removal of methylene blue by adsorption on various carbons—A comparative study, Dyes Pigm. 51 (2001) 25–40.